Nanofaceted C/Re(11$\bar{2}$1): Fabrication, Structure, and Template for Synthesizing Nanostructured Model Pt Electrocatalyst for Hydrogen Evolution Reaction

Xiaofang Yang,[†] Bruce E. Koel,[†] Hao Wang,[‡] Wenhua Chen,[§,*] and Robert A. Bartynski[§]

[†]Department of Chemical and Biological Engineering, Princeton University, Princeton, New Jersey 08544, United States, [‡]Department of Chemistry, Columbia University, New York, New York 10027, United States, and [§]Department of Physics and Astronomy, and Laboratory for Surface Modification, Rutgers, The State University of New Jersey, Piscataway, New Jersey 08854, United States

ABSTRACT

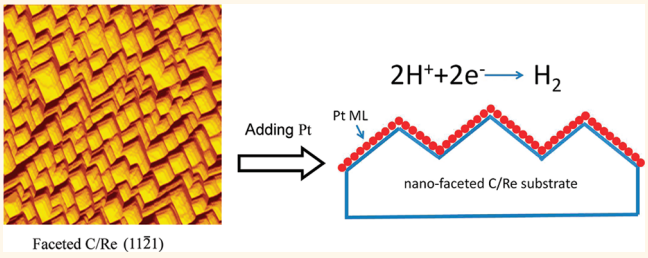

We report the first observation of carbon-induced nanofaceting of a Re single crystal and its application in synthesizing a nanostructured model Pt electrocatalyst investigated using multiple surface science techniques, including low-energy electron diffraction, Auger electron spectroscopy, X-ray photoelectron spectroscopy, low-energy ion scattering, and scanning tunneling microscopy, combined with electrochemical reaction measurements. Upon annealing in acetylene at 700 K followed by annealing in vacuum at 1100 K, an initially planar Re(11$\bar{2}$1) surface becomes completely faceted and covered with three-sided nanopyramids exposing (01$\bar{1}$1), (10$\bar{1}$1), and (11$\bar{2}$0) faces. Using the faceted C/Re(11$\bar{2}$1) surface as a template, we have successfully fabricated a nanostructured Pt monolayer (ML) electrocatalyst. The Pt ML supported on the C/Re nanotemplate exhibits higher activity for the hydrogen evolution reaction than Pt(111). This is the first application of faceted metal surfaces as templates for synthesis of nanoscale model electrocatalyst with well-defined (facet) surface structure and controlled (facet) size on the nanometer scale, illustrating the potential for future studies of nanostructured bimetallic systems relevant to electrocatalytic reactions.

KEYWORDS: rhenium · faceting · carbon · platinum · nanostructure · electrocatalysis

Adsorbate-induced faceting of surfaces is a form of self-assembly on the nanometer scale that has been studied for several decades.[1−8] Faceting is a thermodynamically driven but kinetically limited process. Faceting of initially planar surfaces is facilitated by the adsorption of gases and metals that enhance the anisotropy of the surface free energy.[4,6,7] There are extensive studies of faceting for gas/metal systems,[6,7,9−12] whereas there are only a few investigations of faceting for metal/metal systems.[1,7,13−17] Faceted metal surfaces have been utilized for probing structural and size effects in catalytic reactions[18−20] and as nanotemplates for growth of metallic nanoparticles.[21,22]

The hydrogen evolution reaction (HER) is one of the most extensively studied electrochemical reactions.[23−30] This reaction is of increasing interest as a route to carbon-free generation of H_2 and has great promise for use in the future for automobiles.[25,28,29,31,32] Pt is commonly used as an electrocatalyst for the HER. However, due to the high cost and limited supply of Pt, considerable effort has recently been devoted to the exploration of new HER catalysts that minimize the amount of Pt needed.[28,29,32] Of particular interest is the use of Pt monolayer (ML) catalysts for the HER in order to substantially reduce the Pt loading.[28] For example, it was found that the activity of a Pt ML supported on planar tungsten carbide (WC) shows the same HER activity as bulk Pt.[28]

Rhenium is mainly used in the aircraft industry and in catalysts for petroleum processing.[33] Recently, Re has received increasing attention due to its high reactivity in many important catalytic reactions such as selective reduction of NO_x with NH_3,[34] selective oxidation of methanol,[35,36] thiophene hydrodesulfurization,[37] and ammonia synthesis[38,39] where the reaction rate is sensitive to the catalyst surface structure. In the work presented here, we investigated carbon-induced nanofaceting of a Re(11$\bar{2}$1) single-crystal substrate as part of our larger interest in the influence of carbon on the

* Address correspondence to wchen@physics.rutgers.edu.

Received for review October 31, 2011 and accepted January 22, 2012.

Published online January 22, 2012
10.1021/nn204615j

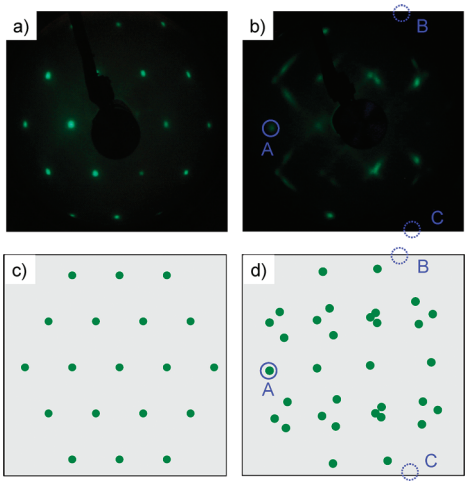

Figure 1. (a) LEED pattern at 60 eV from a clean Re(11$\bar{2}$1) surface; (b) LEED pattern at 60 eV from a faceted C/Re (11$\bar{2}$1) surface prepared by dosing 0.3 L of C_2H_2 at 700 K followed by annealing at 1100 K; (c) kinematical simulation of (a); and (d) kinematical simulation of (b).

surface structure of Re(11$\bar{2}$1). Such a study is of practical importance since carbon is one of the most common impurities in metal-based heterogeneous catalysts. This work is part of an ongoing study that previously addressed O- and N-induced faceting of Re(11$\bar{2}$1).[7,21] We have now found that the presence of surface carbon on Re(11$\bar{2}$1), if followed by annealing in vacuum, causes faceting of Re(11$\bar{2}$1); that is, an initially planar Re(11$\bar{2}$1) surface becomes "nanotextured" to expose new crystal faces on the nanometer scale. The faceted C/Re(11$\bar{2}$1) surface is then used as a nanotemplate to synthesize a Pt ML electrocatalyst, which can serve as a nanoscale model Pt electrocatalyst to bridge the gap between Pt single crystals and supported Pt nanoparticles since a Pt monolayer supported on a faceted C/Re(11$\bar{2}$1) substrate has a well-defined surface structure and controlled facet size on the nanometer scale. We also demonstrate that a Pt ML supported on faceted C/Re(11$\bar{2}$1) exhibits higher activity than a bulk Pt(111) surface for the HER.

RESULTS

Carbon-Induced Nanofaceting of Re(11$\bar{2}$1). Figure 1a shows a LEED pattern at an incident electron energy (E_e) of 60 eV from the clean Re(11$\bar{2}$1) surface. The sharp spots with low background intensity indicate that the surface is highly ordered. Furthermore, when E_e was increased, all of the diffraction spots converged toward the center of the LEED screen, indicating that the surface was macroscopically planar. Upon dosing C_2H_2 on clean Re(11$\bar{2}$1) at 700 K followed by annealing in UHV at 1100 K, which leads to a C-covered surface due to thermal decomposition of C_2H_2 on Re, the LEED spots from the planar surface completely disappeared and instead new LEED spots appeared (Figure 1b). Moreover, these new diffraction spots

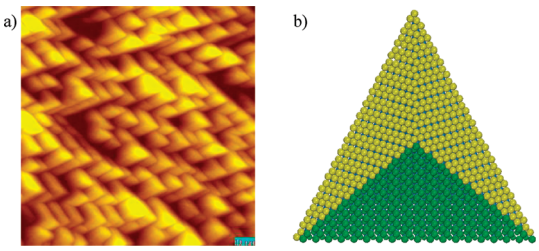

Figure 2. (a) STM image of a faceted C/Re(11$\bar{2}$1) surface prepared by dosing 0.3 L of C_2H_2 at 700 K followed by annealing at 1100 K; and (b) hard sphere model of a single pyramid from the faceted C/Re(11$\bar{2}$1) surface.

did not converge to the screen center but moved toward three distinct points marked by circles A, B, and C when E_e increased (note: circles B and C are located just outside of the LEED screen). The three fixed points are specular beams from three different facets that are macroscopically tilted with respect to the planar Re(11$\bar{2}$1) surface. The LEED pattern from the faceted surface is a superposition of the three sets of LEED patterns that originate from the three tilted surface planes. The spots were less sharp compared to those from the planar surface, which is due to the small finite size of the facets. It is well-known that the size of LEED spots changes with facet size, and the bigger the facet size, the sharper the LEED spots.[18,42] The orientations of the three facets were determined as (01$\bar{1}$1), (10$\bar{1}$1), and (11$\bar{2}$0) on the basis of the three specular beam positions,[21] where A is (11$\bar{2}$0) and B and C are (01$\bar{1}$1) and (10$\bar{1}$1), respectively. Comparison of simulated LEED patterns at several incident electron energies with the corresponding LEED patterns observed experimentally confirms this conclusion, and for example, kinematical simulations of LEED patterns for the planar (Figure 1a) and faceted (Figure 1b) surfaces are shown in Figure 1c and Figure 1d, respectively.

Figure 2a shows a representative scanning tunneling microscopy (STM) image from a faceted C/Re(11$\bar{2}$1) surface prepared by dosing 0.3 L of C_2H_2 at 700 K followed by annealing at 1100 K for 1 min. The surface was completely covered by three-sided pyramids, in agreement with LEED measurements. The three-sided pyramids shown in Figure 2a have a narrow size distribution with an average side width of ~10 nm, which changes with annealing temperature. Figure 2b shows a hard sphere model of a single pyramid of the faceted surface.

Carbon-induced faceting has not been reported previously on any Re surface. This has important implications for Re-based heterogeneous catalysts that operate under carbon-rich conditions since the structure of catalyst surfaces often affects their performance. It should be noted that the C-induced faceting of Re(11$\bar{2}$1) presented here occurs at low carbon coverage (~0.35 ML) as determined by auger electron spectroscopy (AES). The exploration of the possible formation of rhenium carbide at high

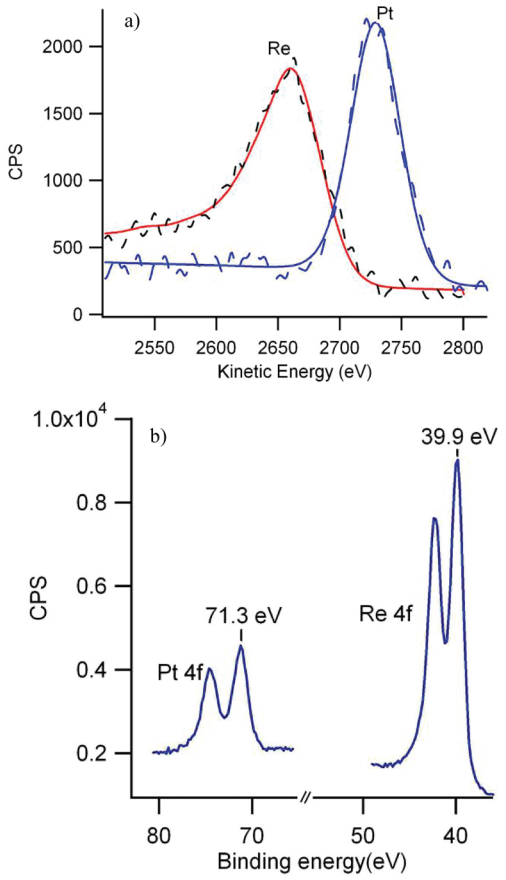

Figure 3. Surface characterization of a Pt monolayer supported on the faceted C/Re(11$\bar{2}$1) surface by LEIS (a) and XPS (b). In (a), the red curve was taken from a clean Re(11$\bar{2}$1) surface; LEIS conditions were 4.5 keV Ar^+, 3.0 nA.

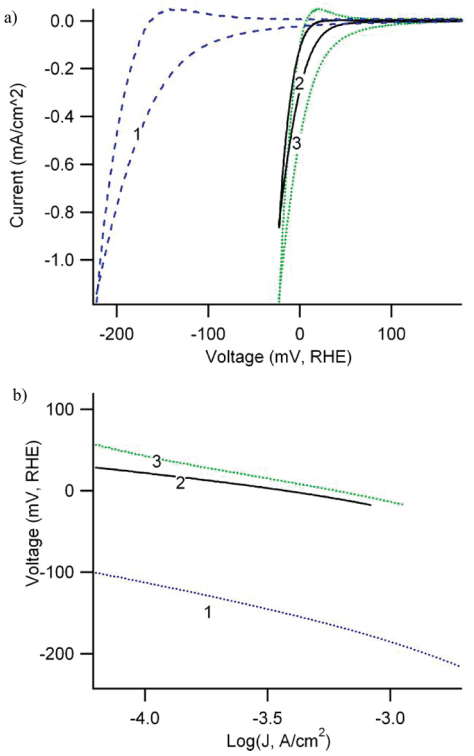

Figure 4. (a) HER polarization curves of (1) Re(11$\bar{2}$1), (2) Pt(111), and (3) Pt ML supported on faceted C/Re(11$\bar{2}$1), in Ar-purged 0.1 M $HClO_4$; and (b) corresponding Tafel plots for the data in (a). The scan rate in the polarization measurements was 2 mV/s.

coverage and high annealing temperature is of interest and will be the subject of future studies since it is known that transition metal carbides have important catalytic properties themselves.[43] For our purposes herein, faceted C/Re(11$\bar{2}$1) surfaces with a well-defined facet structure and controlled facet size on the nanometer scale can serve well as a nanoscale model catalyst or as a nanotemplate for synthesis of more complex materials and structures.[20]

Pt Monolayer on Faceted C/Re(11$\bar{2}$1). The carbon-induced faceted Re(11$\bar{2}$1) surface discussed above can routinely be prepared *in situ* by annealing during C_2H_2 gas exposure. Using this C/Re surface as a template, a nanoscale model electrocatalyst has been successfully fabricated by evaporating a monolayer of Pt onto this template at room temperature. The Pt coverage was characterized by both LEIS and XPS, as shown in Figure 3. The LEIS spectrum in Figure 3a from the Pt ML on faceted C/Re(11$\bar{2}$1) (blue curve) displays only a Pt peak and a negligible Re peak, whereas the red curve shows only a Re peak in the LEIS spectrum from the clean Re(11$\bar{2}$1) surface. The Pt4f and Re4f core levels in XPS from the Pt ML on faceted C/Re(11$\bar{2}$1) are shown in Figure 3b. After this preparation, the Pt ML/C/Re(11$\bar{2}$1) sample was transferred from the UHV chamber to an electrochemical cell to test its catalytic activity for the HER. Figure 4a shows polarization scans for the HER using Re(11$\bar{2}$1), Pt(111), and Pt ML/C/Re(11$\bar{2}$1) samples, which were performed in an Ar-purged 0.1 M $HClO_4$ solution at room temperature with a scan rate of 2 mV/s. Figure 4b gives plots of the HER overpotentials as a function of the logarithm of the exchange current density to produce the corresponding set of Tafel curves. Clearly, the activity of Re(11$\bar{2}$1) for the HER is much lower than Pt(111) as evidenced by the large overpotential. However, the Pt ML/C/Re(11$\bar{2}$1) sample has a significantly improved activity with even better performance than Pt(111). The exchange current (j_0) values for Pt ML/C/Re(11$\bar{2}$1) and Pt(111) are 6.30×10^{-4} and 3.98×10^{-4} A/cm^2, respectively.

DISCUSSION

The enhanced HER activity of the Pt ML/C/Re(11$\bar{2}$1) sample likely has its origin in the electronic structure of the Pt film. When a metal monolayer (ML) resides on the surface of another metal, the d-band center of the overlayer metal typically changes. The energy position of the d-band center of the metal monolayer depends upon the relative electronegativities of the monolayer and substrate metals and affects the binding energy of both atomic and molecular adsorbates.[44−46] In studies of the oxygen reduction reaction (ORR), an

electrochemical reaction occurring at the cathode electrode, a volcano-type dependence of the reaction rate on the center of the d-bands is observed for Pt MLs on different metal substrates.[47] The Pt monolayer on Pd(111) is at the top of the volcano curve with higher ORR activity than both Pt(111) and Pt MLs on other single-crystal metals.[47] Similar volcano type of relationships exists between the hydrogen binding energy (HBE) and HER exchange current density. Such volcano curves are consistent with Pt being the most efficient electrocatalyst for the HER.[31] Greeley *et al.* have found that for a Pd ML on Pt/Ru, which has a HBE value located at the center of the volcano curve, a higher HER exchange current density is found compared to pure Pt and Pd MLs on other metal substrates.[25] Recently, Esposito and co-workers have shown that a Pt ML on WC has an HBE that is similar to that on Pt(111) and thus shows HER activity comparable to that of the single-crystal platinum surface.[28] Therefore, the much lower HER activity of Re(11$\bar{2}$1) compared to Pt(111) is most likely due to the much stronger HBE on Re(11$\bar{2}$1) than on Pt(111).[31] The origin of higher HER activity of Pt ML/C/Re(11$\bar{2}$1) than Pt(111) may be due to a substantially reduced HBE on Pt ML/C/Re(11$\bar{2}$1) compared to that on Re(11$\bar{2}$1). One might expect this to be affected by the amount of carbon, and density functional theory (DFT) calculations of the HBE on Pt-ML/C/Re(11$\bar{2}$1) with different carbon concentrations would provide insight into the origin of the enhanced HER activity of Pt-ML/C/Re(11$\bar{2}$1) surfaces.

Faceting is well-known to affect the chemical activity of a surface. Using Monte Carlo simulations, Persson *et al.* investigated the interplay between reactions occurring on adjacent facets of nanometer-sized supported catalyst particles.[48] These results indicate that the reaction kinetics on faceted nanocrystals can be remarkably different from those on single-crystal surfaces due to nontrivial coupling of the kinetics on the individual facets. Earlier experimental studies of acetylene reactions on planar Pd/W(111) and faceted Pd/W(111) surfaces with varying facet sizes, as well as on a planar Pd/W(211) surface, revealed the important effects of geometric structure and finite size at the nanometer scale on reactions.[49] Notably, unlike the faceted W(111) surface induced by Pd, which consists of three-sided pyramidal facets having only {211} faces,[50] the Pt ML on faceted C/Re(11$\bar{2}$1) has facets with two different kinds of faces (two {01−11} faces and one (11$\bar{2}$0) face). The presence of two faces on the nanometer scale may make it more difficult to explain the effects on the HER due to kinetic competition and finite size effects.[51]

LEIS studies revealed that when faceting of a metal/metal system occurs, the overlayer metal is thermally stable and "floats" on the outer surface of the faceted substrate.[52] A good example is Pt-induced faceting of W(111) and Mo(111).[52,53] However, no evidence was found for Pt-induced faceting of Re(12$\bar{3}$1), another atomically rough Re surface.[54] This may be attributed to intermixing between Pt and Re, which was observed by synchrotron-based high-resolution photoemission spectroscopy (HRPES) (unpublished data). Therefore, Pt-induced faceting of Re(11$\bar{2}$1) under our experimental conditions is unlikely. A detailed spectroscopic and microscopic characterization of the Pt monolayer on faceted C/Re(11$\bar{2}$1) surfaces as a function of carbon coverage will be the subject of future studies to elucidate the role of carbon in stabilizing the Pt monolayer on faceted C/Re(11$\bar{2}$1) substrates.

CONCLUSION

We report our observations of carbon-induced nanofaceting of Re(11$\bar{2}$1), which is unprecedented on a rhenium surface. Dosing C_2H_2 on Re(11$\bar{2}$1) at 700 K followed by annealing at 1100 K causes faceting of Re(11$\bar{2}$1) to form three-sided nanopyramids exposing (01$\bar{1}$1), (10$\bar{1}$1), and (11$\bar{2}$0) faces. Using the faceted C/Re(11$\bar{2}$1) substrate as a nanotemplate, we have successfully synthesized nanoscale model electrocatalysts composed of one monolayer of Pt supported on this surface. The Pt ML on the faceted C/Re(11$\bar{2}$1) surface exhibited higher activity for HER than Pt(111). This is the first report on the application of a faceted metal surface as a template for synthesis of nanoscale model Pt electrocatalysts with well-defined facet surface structure and controlled facet size on the nanometer scale.

EXPERIMENTS

The experiments were conducted in either one or the other of two ultrahigh vacuum (UHV) chambers with base pressures of 2×10^{-10} Torr.[40,41] The same Re(11$\bar{2}$1) and Pt(111) crystals were used for all experiments. A Re(11$\bar{2}$1) crystal was used to prepare both a clean planar Re(11$\bar{2}$1) surface and a C-covered, faceted Re(11$\bar{2}$1) surface. Clean planar Re(11$\bar{2}$1) was prepared by cycles of sputtering (1 keV Ar^+, 5×10^{-6} Torr, 0.4 μA, 5 min) and annealing (1100 K, 2 min). Small oxygen exposures (5×10^{-9} Torr, 1 min) on the sample were also needed to remove surface carbon. A C-covered, faceted Re(11$\bar{2}$1) surface was generated by dosing acetylene (C_2H_2) on the surface at 700 K followed by annealing at 1100 K. The clean Pt(111) surface was also prepared by cycles of sputtering (1 keV Ar^+, 5×10^{-6} Torr, 0.4 μA, 5 min) and annealing (1100 K, 2 min). AES was used to verify the surface cleanliness and the surface carbon coverage. Low-energy electron diffraction (LEED) and scanning tunneling microscopy (STM) were used to monitor the surface structure. Pt was deposited on C-covered faceted Re(11$\bar{2}$1) by physical vapor deposition, and the presence and coverage of surface Pt were characterized by low-energy ion scattering (LEIS) and X-ray photoelectron spectroscopy (XPS). C_2H_2 (99.96% purity, Matheson) was purified by passing it through a dry ice/acetone cold trap. Research-purity O_2 was used without further purification.

All dosing was carried out by backfilling the chambers. All gas exposures are given in Langmuirs (1 Langmuir = 1×10^{-6} Torr·s) and are uncorrected for ion gauge sensitivities.

After surface preparation in the UHV chamber, the crystal was transferred to an electrochemical cell for electrochemical analysis.[40,41] Quick transfer of the sample between the main UHV chamber and the electrochemical cell was accomplished with the aid of a small high-pressure antechamber/load lock attached directly to the UHV chamber. Before sample transfer, this antechamber was filled with high-purity N_2 (99.998% purity, Airgas) to a pressure of 1.5 atm and a small flow of N_2 gas was maintained during sample transfer. The UHV-prepared Pt monolayer supported on the faceted C/Re(11$\bar{2}$1) substrate, denoted as Pt ML/C/Re(11$\bar{2}$1), was protected by placing a droplet of high-purity water (HPLC grade, Fisher) on the surface immediately after opening the port to the antechamber and then immediately transferred into an electrochemical cell and immersed in a 0.1 M $HClO_4$ solution for electrochemical measurements. Here, 1 ML refers to one physical ML that is defined as the coverage needed to shadow all substrate atoms. One physical ML on Re(01$\bar{1}$1) or Re(10$\bar{1}$1) = 2 geometrical MLs = 1.43×10^{15} atoms/cm^2; 1 physical ML on Re(11$\bar{2}$0) = 2 geometrical MLs = 1.88×10^{15} atoms/cm^2; 1 physical ML on Re(11$\bar{2}$1) = 4 geometrical MLs = 1.79×10^{15} atoms/cm^2. However, if we consider a three-sided pyramid covered by one physical ML of Pt on all of the three facets, the density of Pt per projected unit area on (11$\bar{2}$1) is the same as 1 physical ML on planar Re(11$\bar{2}$1). A hanging meniscus rotating disk technique was used and the height of the meniscus was carefully controlled to prevent wetting the side of the crystal. A standard three-electrode electrochemical cell with a Pt wire counter electrode and a hydrogen reference electrode was used.

Conflict of Interest: The authors declare no competing financial interest.

Acknowledgment. B.E.K. acknowledges support of this work by the National Science Foundation (Grant No. CHE-1129417). W.C. and R.A.B. acknowledge support of this work by the U.S. Department of Energy, Office of Basic Energy Sciences (Grant No. DE-FG02-93ER14331).

REFERENCES AND NOTES

1. Cetronio, A.; Jones, J. P. Reconstruction at a Metallic Interface Studied by Field Ion and Field Emission Microscopy. *Surf. Sci.* **1973**, *40*, 227–248.
2. Zhang, C.; van Hove, M. A.; Somorjai, G. A. The Interaction of Oxygen with the Mo(100) and Mo(111) Single-Crystal Surfaces: Chemisorption and Oxidation at High Temperatures. *Surf. Sci.* **1985**, *149*, 326–340.
3. Somorjai, G. A.; Van Hove, M. A. Adsorbate-Induced Restructuring of Surfaces. *Prog. Surf. Sci.* **1989**, *30*, 201–231.
4. Williams, E. D.; Bartelt, N. C. Thermodynamics of Surface Morphology. *Science* **1991**, *251*, 393–400.
5. Reiter, S.; Taglauer, E. Oxygen-Induced Faceting on Cu-(115). *Surf. Sci.* **1996**, *367*, 33–39.
6. Chen, Q.; Richardson, N. V. Surface Facetting Induced by Adsorbates. *Prog. Surf. Sci.* **2003**, *73*, 59–77.
7. Madey, T. E.; Chen, W.; Wang, H.; Kaghazchi, P.; Jacob, T. Nanoscale Surface Chemistry over Faceted Substrates: Structure, Reactivity and Nanotemplates. *Chem. Soc. Rev.* **2008**, *37*, 2310–2327.
8. Szczepkowicz, A. Oxygen-Covered Tungsten Crystal Shape: Time Effects, Equilibrium, Surface Energy and the Edge-Rounding Temperature. *Surf. Sci.* **2011**, *605*, 1719–1725.
9. Sander, M.; Imbihl, R.; Schuster, R.; Barth, J. V.; Ertl, G. Microfacetting of Pt(210) Induced by Oxygen Adsorption and by Catalytic CO Oxidation. *Surf. Sci.* **1992**, *271*, 159–169.
10. Wang, H.; Chan, A. S. Y.; Chen, W.; Kaghazchi, P.; Jacob, T.; Madey, T. E. Facet Stability in Oxygen-Induced Nanofaceting of Re(12−31). *ACS Nano* **2007**, *1*, 449–455.
11. Kaghazchi, P.; Jacob, T.; Ermanoski, I.; Chen, W.; Madey, T. E. First-Principles Studies on Oxygen-Induced Faceting of Ir(210). *ACS Nano* **2008**, *2*, 1280–1288.
12. Shen, Q.; Chen, W.; Wang, H.; Govind; Madey, T. E.; Bartynski, R. A. Nano-Faceting of the Ru(11−20) Surface. *Surf. Sci.* **2010**, *604*, L12–L15.
13. Song, K. J.; Demmin, R. A.; Chengzhi, D.; Garfunkel, E.; Madey, T. E. Faceting Induced by an Ultrathin Metal Film: Pt on W(111). *Surf. Sci.* **1990**, *227*, L79–L85.
14. Song, K. J.; Dong, C. Z.; Madey, T. E. Faceting of Tungsten-(111) Induced by Ultrathin Palladium Films. *Langmuir* **1991**, *7*, 3019–3026.
15. Kolthoff, D.; Dullweber, T.; Pfnür, H. Adsorbate-Induced Faceting of a nearly Close-Packed Surface: Te−Pd(100). *Surf. Sci.* **2000**, *447*, 259–271.
16. Szczepkowicz, A.; Ciszewski, A.; Bryl, R.; Oleksy, C.; Nien, C.-H.; Wu, Q.; Madey, T. E. A Comparison of Adsorbate-Induced Faceting on Flat and Curved Crystal Surfaces. *Surf. Sci.* **2005**, *599*, 55–68.
17. Coati, A.; Creuze, J.; Garreau, Y. Adsorbate-Induced Faceting: The Case of Ag on Vicinal Cu Surfaces. *Phys. Rev. B* **2005**, *72*, 115424.
18. Chen, W.; Ermanoski, I.; Madey, T. E. Decomposition of Ammonia and Hydrogen on Ir Surfaces: Structure Sensitivity and Nanometer-Scale Size Effects. *J. Am. Chem. Soc.* **2005**, *127*, 5014–5015.
19. Chen, W.; Madey, T. E.; Stottlemyer, A. L.; Chen, J. G.; Kaghazchi, P.; Jacob, T. Structure Sensitivity in Adsorption and Decomposition of NO on Ir. *J. Phys. Chem. C* **2008**, *112*, 19113–19120.
20. Chen, W.; Shen, Q.; Bartynski, R. A.; Kaghazchi, P.; Jacob, T. Reduction of NO by CO on Unsupported Ir: Bridging the Materials Gap. *ChemPhysChem* **2010**, *11*, 2515–2520.
21. Wang, H. Adsorbate-Induced Nanoscale Faceting of Rhenium Surfaces, Ph.D. Thesis, Rutgers University, 2008.
22. Shen, Q.; Chen, W.; Bartynski, R. A. Growth of Gold Nanoparticles on Faceted O/Ru(11−20) Nanotemplate. *Surf. Sci.* **2011**, *605*, 1457–1461.
23. Hinnemann, B.; Moses, P. G.; Bonde, J.; Jørgensen, K. P.; Nielsen, J. H.; Horch, S.; Chorkendorff, I.; Nørskov, J. K. Biomimetic Hydrogen Evolution: MoS_2 Nanoparticles as Catalyst for Hydrogen Evolution. *J. Am. Chem. Soc.* **2005**, *127*, 5308–5309.
24. Greeley, J.; Jaramillo, T. F.; Bonde, J.; Chorkendorff, I.; Norskov, J. K. Computational High-Throughput Screening of Electrocatalytic Materials for Hydrogen Evolution. *Nat. Mater.* **2006**, *5*, 909–913.
25. Greeley, J.; Nørskov, J. K.; Kibler, L. A.; El-Aziz, A. M.; Kolb, D. M. Hydrogen Evolution over Bimetallic Systems: Understanding the Trends. *ChemPhysChem* **2006**, *7*, 1032–1035.
26. Jaramillo, T. F.; Jørgensen, K. P.; Bonde, J.; Nielsen, J. H.; Horch, S.; Chorkendorff, I. Identification of Active Edge Sites for Electrochemical H_2 Evolution from MoS_2 Nanocatalysts. *Science* **2007**, *317*, 100–102.
27. Norskov, J. K.; Bligaard, T.; Rossmeisl, J.; Christensen, C. H. Towards the Computational Design of Solid Catalysts. *Nat. Chem.* **2009**, *1*, 37–46.
28. Esposito, D. V.; Hunt, S. T.; Stottlemyer, A. L.; Dobson, K. D.; McCandless, B. E.; Birkmire, R. W.; Chen, J. G. Low-Cost Hydrogen-Evolution Catalysts Based on Monolayer Platinum on Tungsten Monocarbide Substrates. *Angew. Chem., Int. Ed.* **2010**, *49*, 9859–9862.
29. Bjorketun, M. E.; Bondarenko, A. S.; Abrams, B. L.; Chorkendorff, I.; Rossmeisl, J. Screening of Electrocatalytic Materials for Hydrogen Evolution. *Phys. Chem. Chem. Phys.* **2010**, *12*, 10536–10541.
30. Li, Y.; Wang, H.; Xie, L.; Liang, Y.; Hong, G.; Dai, H. MoS_2 Nanoparticles Grown on Graphene: An Advanced Catalyst for the Hydrogen Evolution Reaction. *J. Am. Chem. Soc.* **2011**, *133*, 7296–7299.
31. Norskov, J. K.; Bligaard, T.; Logadottir, A.; Kitchin, J. R.; Chen, J. G.; Pandelov, S.; Stimming, U. Trends in the Exchange Current for Hydrogen Evolution. *J. Electrochem. Soc.* **2005**, *152*, J23–J26.
32. Stephens, I. E. L.; Chorkendorff, I. Minimizing the Use of Platinum in Hydrogen-Evolving Electrodes. *Angew. Chem., Int. Ed.* **2011**, *50*, 1476–1477.

33. Naumov, A. V. Rhythms of Rhenium. *Russ. J. Non-Ferrous Metals* **2007**, *48*, 418–423.
34. Wachs, I. E.; Deo, G.; Andreini, A.; Vuurman, M. A.; de Boer, M. The Selective Catalytic Reduction of NO_x with NH_3 over Titania Supported Rhenium Oxide Catalysts. *J. Catal.* **1996**, *160*, 322–325.
35. Yuan, Y.; Shido, T.; Iwasawa, Y. The New Catalytic Property of Supported Rhenium Oxides for Selective Oxidation of Methanol to Methylal. *Chem. Commun.* **2000**, 1421–1422.
36. Liu, J.; Zhan, E.; Cai, W.; Li, J.; Shen, W. Methanol Selective Oxidation to Methyl Formate over ReO_x/CeO_2 Catalysts. *Catal. Lett.* **2008**, *120*, 274–280.
37. Bussell, M. E.; Gellman, A. J.; Somorjai, G. A. Thiophene Hydrodesulfurization over Transition Metal Surfaces: Structure Insensitive over Molybdenum and Structure Sensitive over Rhenium. *J. Catal.* **1988**, *110*, 423–426.
38. Asscher, M.; Carrazza, J.; Khan, M. M.; Lewis, K. B.; Somorjai, G. A. The Ammonia Synthesis over Rhenium Single-Crystal Catalysts: Kinetics, Structure Sensitivity, and Effect of Potassium and Oxygen. *J. Catal.* **1986**, *98*, 277–287.
39. Kojima, R.; Enomoto, H.; Muhler, M.; Aika, K.-i. Cesium-Promoted Rhenium Catalysts Supported on Alumina for Ammonia Synthesis. *Appl. Catal., A* **2003**, *246*, 311–322.
40. Yang, X.; Hu, J.; Wu, R.; Koel, B. E. Formation of Pd Monomers and Dimers on a Single-Crystal $Pd_3Fe(111)$ Surface. *J. Phys. Chem. Lett.* **2010**, *1*, 2493–2497.
41. Yang, X.; Hu, J.; Fu, J.; Wu, R.; Koel, B. E. Role of Surface Iron in Enhanced Activity for the Oxygen Reduction Reaction on a $Pd_3Fe(111)$ Single-Crystal Alloy. *Angew. Chem., Int. Ed.* **2011**, *50*, 10182–10185.
42. Ermanoski, I.; Pelhos, K.; Chen, W.; Quinton, J. S.; Madey, T. E. Oxygen-Induced Nano-Faceting of Ir(210). *Surf. Sci.* **2004**, *549*, 1–23.
43. Hwu, H. H.; Chen, J. G. Surface Chemistry of Transition Metal Carbides. *Chem. Rev.* **2004**, *105*, 185–212.
44. Hammer, B.; Nørskov, J. K. Electronic Factors Determining the Reactivity of Metal Surfaces. *Surf. Sci.* **1995**, *343*, 211–220.
45. Hammer, B.; Nørskov, J. K. Theoretical Surface Science and Catalysis—Calculations and Concepts. In *Advances in Catalysis*; Bruce, C., Gates, H. K., Eds.; Academic Press: New York, 2000; Vol. 45, pp 71−129.
46. Chen, J. G.; Menning, C. A.; Zellner, M. B. Monolayer Bimetallic Surfaces: Experimental and Theoretical Studies of Trends in Electronic and Chemical Properties. *Surf. Sci. Rep.* **2008**, *63*, 201–254.
47. Zhang, J.; Vukmirovic, M. B.; Xu, Y.; Mavrikakis, M.; Adzic, R. R. Controlling the Catalytic Activity of Platinum-Monolayer Electrocatalysts for Oxygen Reduction with Different Substrates. *Angew. Chem., Int. Ed.* **2005**, *44*, 2132–2135.
48. Persson, H.; Thormahlen, P.; Zhdanov, V. P.; Kasemo, B. Monte Carlo Simulations of the Kinetics of Catalytic Reactions on Nanometer-Sized Particles, with Diffusion over Facet Boundaries. *J. Vac. Sci. Technol., A* **1999**, *17*, 1721–1726.
49. Barnes, R.; Abdelrehim, I. M.; Madey, T. E. Structure Sensitivity in Acetylene Reactions over Bimetallic Pd/W Surfaces. *Top. Catal.* **2000**, *14*, 53–61.
50. Nien, C. H.; Madey, T. E. Atomic Structures on Faceted W(111) Surfaces Induced by Ultrathin Films of Pd. *Surf. Sci.* **1997**, *380*, L527–L532.
51. Zhdanov, V. P.; Kasemo, B. Simulations of the Reaction Kinetics on Nanometer Supported Catalyst Particles. *Surf. Sci. Rep.* **2000**, *39*, 25–104.
52. Dong, C.; Zhang, L.; Diebold, U.; Madey, T. E. A Search for Surface Alloy Formation in Faceting Induced by Monolayer Metal Films: Pd/W (111) and Ni/W (111). *Surf. Sci.* **1995**, *322*, 221–229.
53. Madey, T. E.; Guan, J.; Nien, C.-H.; Dong, C.-Z.; Tao, H.-S.; Campbell, R. A. Faceting Induced by Ultrathin Metal Films on W(111) and Mo(111): Structure, Reactivity, and Electronic Properties. *Surf. Rev. Lett.* **1996**, *3*, 1315–1328.
54. Wang, H.; Chen, W.; Madey, T. E. Morphological Evolution in Oxygen-Induced Faceting of Re(12−31). *Phys. Rev. B* **2006**, *74*, 205426.